Additive Manufacturing 30 (2019) 100841

Contents lists available at ScienceDirect

Additive Manufacturing

journal homepage: www.elsevier.com/locate/addma

Evaluating the coefficient of thermal expansion of additive manufactured AlSi10Mg using microwave techniques

Richard Gumbleton[a,*], Jerome A. Cuenca[b], Georgina M. Klemencic[b], Nick Jones[c], Adrian Porch[a]

[a] School of Engineering, Cardiff University, CF24 3AA, UK
[b] School of Physics and Astronomy, Cardiff University, CF24 3AA, UK
[c] Renishaw Plc, Wotton-under-Edge GL12 8JR, UK

ARTICLE INFO

Keywords:
Thermal expansion
CTE
Powder bed fusion
Microwave
AlSi10Mg

ABSTRACT

In this paper we have used laser powder bed fusion (PBF) to manufacture and characterize metal microwave components. Here we focus on a 2.5 GHz microwave cavity resonator, manufactured by PBF from the alloy AlSi10Mg. Of particular interest is its thermal expansion coefficient, especially since many microwave applications for PBF produced components will be in satellite systems where extreme ranges of temperature are experienced. We exploit the inherent resonant frequency dependence on cavity geometry, using a number of TM cavity modes, to determine the thermal expansion coefficient over the temperature range 6–450 K. Our results compare well with literature values and show that the material under test exhibits lower thermal expansion when compared with a bulk aluminium alloy alternative (6063).

1. Introduction

Additive manufacturing (AM) is a modern fabrication process that enables three-dimensional components to be built using multiple two-dimensional layers. AM enables advancements in component manufacture in many fields of engineering, but it is still a relatively new technology where the thermal properties of various alloys need to be explored. Components produced by laser powder bed fusion (PBF, one form of AM) are being utilised in satellite feed chains due to the ability to achieve up to 99.8% density but with a 50% weight reduction compared to the subtractive manufactured equivalents [1], however AM adoption in this field is still in its infancy [2]. PBF offers increased geometrical freedom in terms of the internal design of three-dimensional components [3] as well as drastically reduced lead times for rapid prototyping [4]. The PBF process consists of spreading thin layers of metallic powder which are laser melted into the desired pattern, with each layer contributing to the three-dimensional build. A schematic of the process is shown in Fig. 1.

Thermal expansion can be problematic in many areas of engineering, not least during the PBF process itself where higher silicon content in aluminium alloy powders can help lower thermal expansion and prevent crack formation [5] during the rapid melting and solidification process. In metallic solids, the crystalline structure of atoms is relatively compact at 0 K, but as temperature increases the potential energy and spacing between atoms increases and forces the solid to expand [6]. In one extreme, modern bridges allow for expansion through the use of specially placed expansion joints, where structural restraining forces of the order of 4×10^6 N would otherwise be required to prevent loss of support in the presence of only a 10 K temperature rise [7]. Similarly, thermal expansion can have detrimental effects during precision engineering. High frequency waveguides and filters, for example, have critical dimensions which are sensitive to temperature, which results in deviations in their desired operating frequencies. Large enough shifts in frequency can render a device inadequate for its intended purpose. This phenomenon is particularly worrisome when operating in harsh temperature environments, such as in space and aerospace applications where, for example, typical thermal cycling between 98 and 433 K is experienced by components of satellite systems [8]. It is therefore apparent that accurate information about the building materials is essential in order to make considered judgments regarding safety and suitability. The metric for quantifying geometrical changes due to changes in temperature is the coefficient of thermal expansion (CTE).

However, metallic AM parts currently show inferior electrical properties when compared to traditional bulk metals due to significant losses at high frequencies arising from poor surface finish [9]. Surface resistance (R_S) in metals at microwave frequencies arises due to the skin effect, where the majority of current is carried in a thin surface layer

* Corresponding author.
E-mail addresses: gumbletonr1@cardiff.ac.uk (R. Gumbleton), cuencaj@cardiff.ac.uk (J.A. Cuenca), georgina.klemencic@astro.cf.ac.uk (G.M. Klemencic), nick.jones@renishaw.com (N. Jones), porcha@cardiff.ac.uk (A. Porch).

https://doi.org/10.1016/j.addma.2019.100841
Received 25 June 2019; Received in revised form 28 August 2019; Accepted 28 August 2019

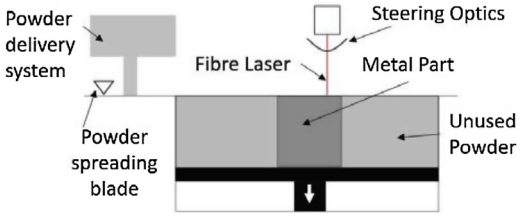

Fig. 1. Schematic of the laser powder bed fusion process.

called the skin depth. For aluminium (of bulk conductivity 2.63×10^7 S/m) the skin depth at 2.5 GHz is calculated to be ≈2 μm, and so even micro surface features can have a significant impact on current flow and hence microwave loss. To overcome these losses, post processing techniques such as machine polishing [10] and silver plating are often employed [9,11,12]. Machine polishing of three dimensional structures is not always possible and silver plating has become the most commonly used treatment. Silver plating, however, is subject to discrepancies between the CTE of different materials where, in these instances, the plating material can disassociate from the AM surface and result in failure [13]. For example, silver has a CTE of $18 \times 10^{-6}\,K^{-1}$ while the CTE of bulk aluminium alloy 6063 is $23 \times 10^{-6}\,K^{-1}$ (between 293 and 393 K) [14,15]. Similar issues are faced with polymer AM processes that require metallic coating [16]. Furthermore, the selection of processing techniques can delivery differing mechanical properties from the same raw material, for example PBF processed AlSi10Mg exhibits a higher tensile strength than cast AlSi10Mg [17]. So although properties of the raw material may be known, the use of AM as a processing technique can bring about alternative properties values. Thus, the investigation of thermal expansion in AM parts is of major interest, and the added advantage of being able to machine complex geometries opens opportunities to use less conventional, but potentially more precise, methods to examine the materials used. This study uses a fractional frequency shift method to evaluate the true CTE of an aluminium cylindrical microwave cavity produced through PBF over a wide temperature range (6–450 K) without the need for strict calibration. To the authors knowledge, this is the first time that CTE has been assessed over a wide range of temperature, as is appropriate for space-based components, using a passive microwave structure (produced by PBF) that can be adopted in a satellite communications system.

2. Measurement theory

A common form of CTE described in literature is the 'mean' CTE [18], a linear average of the expansion of a material over a specified temperature range, expressed as

$$\alpha_m = \frac{1}{L_0}\frac{L_1 - L_0}{T_1 - T_0} \tag{1}$$

where L and T are length and temperature, respectively, while 0 and 1 denote the initial and final values, respectively. Limiting Eq. (1) to infinitesimal changes in length and temperature, we can define the true CTE as

$$\alpha_c \approx \frac{1}{L_0}\frac{\mathrm{dL}}{\mathrm{dT}} \tag{2}$$

where dL/dT is the gradient of the tangent to the curve of length against temperature and is expressed at one temperature point.

A microwave cavity resonator method can be used to obtain the CTE by evaluating the derivative of resonant frequency over temperature. The metallic material of interest must be machined to contain a hollow cavity of known dimensions. The method is based on the microwave resonant frequency response of this cavity being directly dependent on the geometry. The equation for the resonant frequency, f, of transverse-magnetic (TM) modes in a cylindrical air spaced cavity is given by [19]

$$f_{\mathrm{nml}} = \frac{c}{2\pi}\sqrt{\left(\frac{p_{\mathrm{nm}}}{a}\right)^2 + \left(\frac{l\pi}{d}\right)^2} \tag{3}$$

where c is the speed of light, m, n and l are the mode integers, i.e. p_{nm} is mth root of the nth order Bessel function $J_n(x)$ of the first kind, and l is the integer number of half wavelengths along the cavity axis; a and d are the cavity radius and height, respectively. To simplify the analysis, only TM_{nm0} resonant modes are measured, therefore the temperature dependent geometrical term a alone influences the resonant frequency and can be approximated to the first order as

$$a_0(T) \approx a_0(1 + \alpha_c(T - T_0)) \tag{4}$$

where a_0 is the initial radius, α_c is the linear CTE of the cavity walls and T_0 is the initial temperature. Evaluating the first order partial derivatives of Eq. (3), including the temperature dependence of Eq. (4), the true CTE can be expressed as [20,21]

$$\alpha_c \approx -\frac{1}{f_0}\frac{\mathrm{df}}{\mathrm{dT}} \tag{5}$$

for small shifts in f and T. Hence small shifts in resonant frequency can be directly attributed to the CTE of the cavity material.

3. Experimental method

The cylindrical microwave cavity resonator used in this study [22] was produced on a Renishaw AM250 laser powder bed fusion additive manufacturing system. The cavity material, aluminium alloy (AlSi10Mg), comprises aluminium with up to 10% mass fraction of silicon and small quantities of other elements such as magnesium. The silicon present helps to improve the fluidity of the melt pool while the addition of magnesium makes the alloy both harder and stronger than pure aluminium [23]. The chemical constituents of AlSi10Mg are shown in Table 1.

The main PBF process parameters include laser power = 200 W, hatch distance = 130 μm, layer thickness = 25 μm, exposure time = 140 μs and point distance = 80 μm. The equivalent scan speed is 512 mm/s using a meander scan pattern. Each layer is orientated at 67° to the previous layer and the average particle size is 45 μm. The chamber is vacuumed with a flow of argon to avoid oxidisation of the powder.

The TM_{010} mode of the cavity is used to measure the resonant frequency over the temperature range 6–450 K. The TM_{010} mode of a cylindrical cavity is the lowest frequency (i.e. dominant) mode of such a structure when the radius is larger than the length. Its electro-magnetic (EM) field distribution comprises a high electric field on its axis, and high azimuthal magnetic field near to its outer perimeter. Higher order modes, TM_{210} and TM_{310}, are also observed between 310 and 450 K to investigate the influence of the EM field distribution on CTE. The cavity used and the EM field distributions for each mode are shown in Fig. 2. The cavity dimensions were a = 4.6 cm and d = 4.0 cm while the resonant frequencies (at 310 K) of the three modes studied were TM_{010} at 2.522 GHz, TM_{210} at 5.343 GHz and TM_{310} at 6.643 GHz.

To cover such a wide temperature range, the experiment was

Table 1
Chemical composition of AlSi10Mg aluminium powder.

Element	Al	Si	Mg	Fe	N	O	Ti	Zn	Mn	Ni	Cu	Pb	Sn
Mass%	Bal	10	0.35	0.25	0.20	0.20	0.15	0.10	0.10	0.05	0.05	0.02	0.02

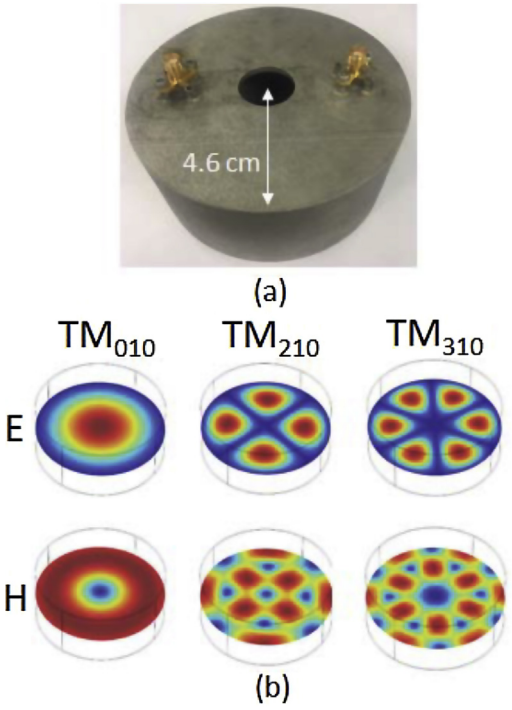

Fig. 2. (a) Cylindrical cavity produced through laser powder bed fusion, (b) electric and magnetic field magnitude distributions of TM_{010}, TM_{210} and TM_{310} modes.

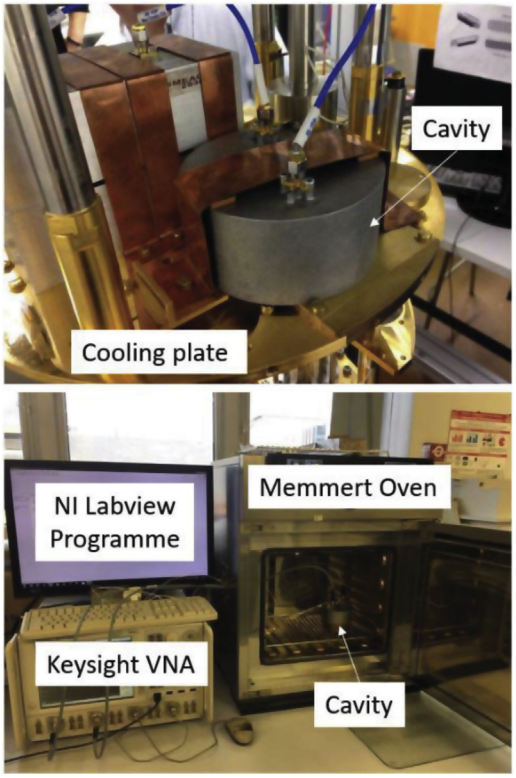

Fig. 3. Photograph of the experimental setup for the dilution fridge (6–300 K) and oven ramps (310–450 K).

conducted in two parts: a cooling ramp between 6 and 300 K and a heating ramp between 310 and 450 K. Fig. 3 shows the two experimental setups used for each section of the temperature range. The fractional frequency shift for both ramps was measured through 2-port S-parameters, with the cooling ramp using a Keysight Fieldfox N9914A portable vector network analyser (VNA) and the heating ramp using a lab based Keysight VNA. Due to a wider available frequency range in the heating ramp setup, higher order modes, TM_{210} and TM_{310}, were also observed between 310 and 450 K to investigate the influence of field magnitudes distribution on CTE. The cooling system used for the low temperature range is a Bluefors dilution fridge with a cooling rate of 0.2 K/min. The AM microwave cavity resonator was clamped to the still plate with copper straps and the temperature of the cavity was directly measured using a calibrated diode thermometer. To ensure good thermal contact with the plate, the rough as-manufactured surface of the cavity was polished until visually smooth. For the high temperature range, the cavity was heated in a Memmert UF 30 oven with a 1 K/min heating rate. A National Instruments (NI) NI-cDAQ-9171 was used to interface two temperature sensors and a NI LabVIEW program was used to record all measurements during the oven ramp. A comparison between the Keysight and Fieldfox VNAs was performed to ensure consistency in frequency measurements. Measurements of the voltage transmission coefficient, S_{21}, taken under the same environmental conditions produced a deviation of $\approx$20 kHz between the resonant frequency of TM_{010} recorded by the two measurements systems. Therefore random errors are very small, less than 0.1% owing to the high precision of frequency measurement, but a systematic error of $\pm$ 1 K in temperature measurement around room temperature results in a $\pm$ 0.3% error in CTE.

4. Results and discussion

The resonant frequency of the PBF produced cylindrical cavity across the full temperature range is shown in Fig. 4. At ~310 K there is a deviation from the trend line in the absolute values of the resonant frequency when comparing the fridge and oven measurements. This is due to the design of the cavity containing a hole at the top and bottom. Since the electric field of the TM_{010} mode is central and parallel to the axis of the cavity, the electric field leaks from the hole. This fringing field will interact with materials external to the cavity, in this instance the copper strip attaching the cavity to the cold plate of the dilution fridge. The exact proximity and material was not replicated in the oven ramp and explains the deviation from the trend line. At temperatures above ~150 K, we observe that the resonant frequency is linearly proportional to the ambient temperature. When cooled to temperatures lower than ~150 K, the resonant frequency starts to saturate and is no longer linearly dependent on temperature, while at temperatures below ~40 K this tends to a constant. The inset of Fig. 4 are S_{21} traces at three temperature points with the corresponding Q factor values. We observe that at lower temperatures the 3 dB bandwidth is narrow with a higher Q factor, relating inversely to electrical resistance. Comparing the measured Q factor values to an equivalent cavity produced via

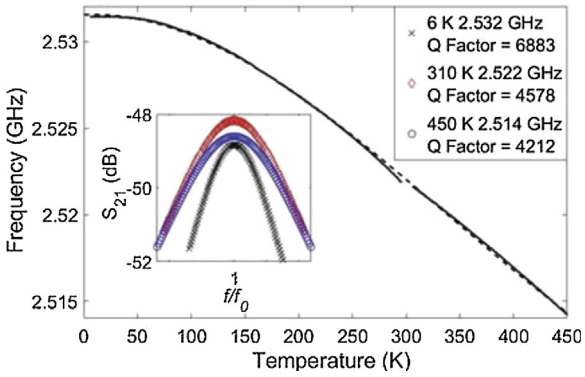

Fig. 4. Resonant frequency shift of TM_{010} as a function of temperature. The dashed line is added as a guide to the eye. Inset plot of normalised S_{21} traces at different temperatures.

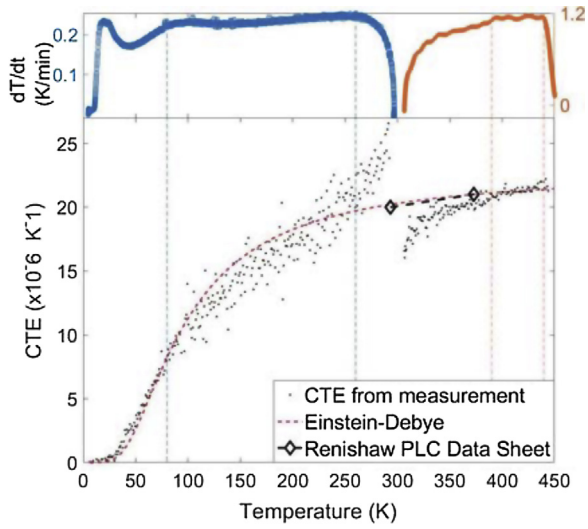

Fig. 5. True linear coefficient of thermal expansion as a function of temperature, derived from the resonant frequency measurements of the cylindrical cavity in TM_{010} mode. The curve fit uses the Einstein–Debye approximation for thermal behavior in solids [25]. The error in CTE owing to temperature measurement is ± 0.3%.

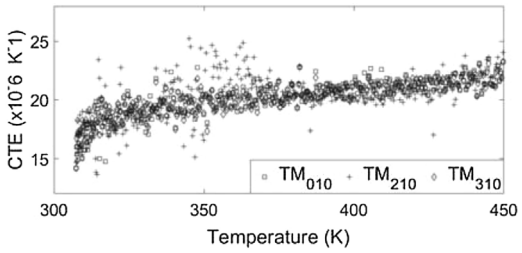

Fig. 6. True linear coefficient of thermal expansion. Derived from resonant frequency measurements for TM_{010}, TM_{210} and TM_{310} cavity modes.

traditional methods ($Q \approx 11{,}000$ at 310 K and $Q \approx 9500$ at 450 K [24]), highlights the significant negative impact that poor surface finish, associated with AM components, has on R_S.

Plotting the gradient of the frequency shift as per Eq. (5) produces a plot of the true CTE, displayed in Fig. 5. The diamond markers indicate the value for CTE specified in the Renishaw PLC datasheet for AlSi10Mg [23], which matches closely with the recorded data and agrees well with the fitted Einstein–Debye curve. Observed CTE values between 260 and 390 K deviate from the curve fit. In addition to the deviation arising from the cavity design, there is also uncertainty due to cooling/heating gradients at the start of each ramp, prior to the material reaching a thermal equilibrium. The inset curves for temperature gradient with respect to time (dT/dt) show periods of non-linearity between 0–80, 260–300, and 310–390 K. However, the Einstein–Debye model [25] provides a good fit in spite of the non-linear regions. CTE at low temperatures exhibits a T^3 thermal dependence and a very low temperatures the vibrations that relate to lattice energy levels, and hence to thermal expansion, starts to freeze out [26] causing CTE to tend to zero. While at high temperatures CTE becomes approximately constant, as per the Dulong–Petit law [26], where it can be observed that CTE values between 293 and 393 K are lower than that stated in literature for bulk aluminium alloy 6063 ($23 \times 10^{-6}\,K^{-1}$) [15]. 6000 series aluminium alloys are commonly utilised in the manufacture of microwave resonant structures due to its high electrical conductivity [27].

Fig. 6 shows the CTE for TM_{010}, TM_{210} and TM_{310} modes between 310 and 450 K. Each measured mode produces a similar CTE curve. This suggests that field distribution within the cavity, at least for low power applications, does not have an effect on CTE and is a good indicator of homogeneity. The results outlined above show the utilisation of a little known microwave technique as an alternative to traditional methods of measuring CTE. The technique demonstrates the use of microwave cavity resonators made from the material under test since they are very susceptible to temperature. Previous studies [20,21] have shown the extraction of CTE using this method for aluminium and copper has been achieved owing to the ability to measure frequency with errors as small as $\sim 10^{-5}$. While this approach requires that the metal be fabricated into a specific geometry, the advantage of AM is that such unconventional shapes can be easily realised. Traditional CTE measurement techniques, such as push rod dilaometry and thermo-mechanical analysis, have also been successfully used to evaluate thermal expansion in PBF materials (Invar36, Stainless steel 316L and Ti-6Al-4V) between 280 and 1200 K [28,29]. Push rod dilatometry [30] uses the linear displacement of a rod placed against the sample under test to evaluate CTE. Thermo-mechanical analysis [31] is closely related to dialometry, however, uses a force equalisation technique to measure changes in length. In both techniques, commercially available equipment can provide a resolution of ~10 nm [32]. A more precise CTE measurement technique is interferometry [33], an optical technique that uses changes in reflected 'fringe' patterns to infer changes in geometry. However, due to the requirement for highly reflective surfaces and complex alignment processes, interferometry is more often utilised to measure the rod displacement in dilalometry systems, culminating in resolutions as small as ~0.25 nm [34]. In all of the above mentioned traditional techniques, strict sample preparation criteria must be observed with sample volume normally required in low cm^3 range while often requiring an additional material of known CTE for calibrating out the CTE of the measurement system itself. The main limitation of this study is the thermal lag present due to non-linear heating and cooling rates, where the cavity fails to reach a thermal equilibrium during the early stages of each temperature ramp. This may be overcome through finer control of the temperature gradients.

5. Conclusion

In conclusion, this study has used a fractional frequency shift method to evaluate the true CTE for PBF AlSi10Mg metal. This technique has allowed the material to be characterized across an extreme temperature range as a functional component, negating the need for calibration pieces and small geometrical material samples. Measured CTE results are found to match well with the CTE value reported in the manufactures data sheet ~ 20–$21 \times 10^{-6}\,K^{-1}$ over the specified temperature range.

Conflict of interest

None declared.

Acknowledgments

R.G. has been supported by the Engineering and Physical Sciences Research Council (EPSRC) and Renishaw Plc via an ICASE studentship programme (EP/R511882/1). J.C. has been supported by EPSRC under the program Grant, GaN-DaME (EP/P00945X/1). G.M.K. has been supported by the European Research Council (ERC) Consolidator Grant 'SUPERNEMS' (647471). Information on the data underpinning the results presented here, including how to access them, can be found in the Cardiff University data catalogue at http://doi.org/10.17035/d.2019.0075533614.

References

[1] N.T. Aboulkhair, N.M. Everitt, I. Ashcroft, C. Tuck, Reducing porosity in AlSi10Mg parts processed by selective laser melting, Addit. Manuf. 1 (2014) 77–86.

[2] H. Williams, E. Butler-Jones, Additive manufacturing standards for space resource utilization, Addit. Manuf. 28 (2019) 676–681.
[3] P.A. Booth, E.V. Lluch, Realising advanced waveguide bandpass filters using additive manufacturing, IET Microwaves Antennas Propag. 11 (14) (2017) 1943–1948.
[4] S.H. Khajavi, J. Partanen, J. Holmström, Additive manufacturing in the spare parts supply chain, Comput. Ind. 65 (1) (2014) 50–63.
[5] A. Maamoun, et al., Thermal post-processing of AlSi10Mg parts produced by selective laser melting using recycled powder, Addit. Manuf. 21 (2018) 234–247.
[6] R. Smallman, R. Bishop, Modern Physical Metallurgy and Materials Engineering, Butteworth-Heinemann, 1999.
[7] D.J. Lee, Bridge Bearings and Expansion Joints, Chapman and Hall, 1994.
[8] J.C. Yang, K.K. de Groh, Materials issues in the space environment, MRS Bull. 35 (1) (2010) 12–20.
[9] P. Booth, E. Valles Lluch, Enhancing the performance of waveguide filters using additive manufacturing, Proc. IEEE 105 (4) (2017) 613–619.
[10] D.L. Creedon, et al., A 3d printed superconducting aluminium microwave cavity, Appl. Phys. Lett. 109 (3) (2016) 032601.
[11] O. Peverini, et al., Selective laser melting manufacturing of microwave waveguide devices, Proc. IEEE 105 (4) (2017) 620–631.
[12] T. Chio, et al., Application of direct metal laser sintering to waveguide-based passive microwave components, antennas, and antenna arrays, Proc. IEEE 105 (4) (2017) 632–644.
[13] D. King, et al., Selective laser melting for the preparation of an ultra-high temperature ceramic coating, Ceram. Int. 45 (2019) 2466–2473.
[14] C.Y. Ho, R. Taylor, Thermal Expansion of Solids, ASM International, 1998.
[15] Atlas-Steels, Aluminium Alloy Data Sheet 6063, Datasheet, Atlas Steels, 2013.
[16] M. Dionigi, et al., Simple high-performance metal-plating procedure for stereolithographically 3-d-printed waveguide components, Microwave Wirel. Comp. Lett. 27 (11) (2017) 953–955.
[17] L. Lam, et al., Phase analysis and microstructure characterisation of alsi10 mg parts produced by selective laser melting, Virt. Phys. Prototyp. 10 (4) (2015) 207–215.
[18] J. James, et al., A review of measurement techniques for the thermal expansion coefficient of metals and alloys at elevated temperatures, Meas. Sci. Technol. 12 (3) (2000) R1–R15.
[19] D. Pozar, Microwave Engineering, Wiley, 1998.
[20] J.A. Cuenca, D. Slocombe, A. Porch, Temperature correction for cylindrical cavity perturbation measurements, IEEE Trans. Microwave Theory Techn. 65 (6) (2017) 2153–2161.
[21] J.A. Cuenca, D. Slocombe, A. Porch, Corrections to 'Temperature correction for cylindrical cavity perturbation measurements', IEEE Trans. Microwave Theory Techn. (2017).
[22] N. Clark, Microwave Methods for Additive Layer Manufacturing, School of Engineering, Cardiff University, 2017 (Ph.D. thesis).
[23] Renishaw-PLC, AlSi10Mg-0403 Powder for Additive Manufacturing, Datasheet, Renishaw PLC, 2015.
[24] N. Clark, G. Shaw, A. Porch, Effect of surface stresses on microwave surface resistance and its impact for cavity perturbation measurements, Microwave Wirel. Comp. Lett. 27 (10) (2017) 939–941.
[25] M. Cankurtaran, B. Askerov, Equation of state, isobaric specific heat and thermal expansion of solids with polyatomic basis in the Einstein–Debye approximation, Phys. Stat. Solidi (B) 194 (1996) 499–507.
[26] N. Ashcroft, N. Mermin, Solid State Physics, Brooks/Cole, 1976.
[27] N. Clark, et al., Particle size characterisation of metals powders for additive manufacturing using a microwave sensor, Powder Technol. 327 (2018) 536–543.
[28] M. Yakout, et al., A study of thermal expansion coefficients and microstructure during selective laser melting of invar 36 and stainless steel 316L, Addit. Manuf. 24 (2018) 409–418.
[29] A. Mertens, et al., Mechanical properties of alloy Ti-6Al-4V and of stainless steel 316L processed by selective laser metling: influence of out-of-equilibrium microstructures, Powder Metall. 57 (3) (2014) 184–189.
[30] ASTM-International, Standard Test Method for Linear Thermal Expansion of Solid Materials with a Push-Rod Dilatometer, Standard, ASTM International, West Conshohocken, 2017.
[31] ASTM-International, Standard Test Method for Linear Thermal Expansion of Solid Materials by Thermomechanical Analysis, Standard, ASTM International, West Conshohocken, 2017.
[32] T. Instruments, Dialtometry-l90016.000, Datasheet, TA Instruments, 2013.
[33] ASTM-International, Standard Test Method for Linear Thermal Expansion of Rigid Solids with Interferometry, Standard, ASTM International, West Conshohocken, 2017.
[34] N. Okaji, et al., Laser interferometic dialtometer at low temperatures: application to fused silica SRM 739, Cryogenics 35 (12) (1995) 887–891.